

# Experimental estimation of a D-shaped cylinder wake using body-mounted sensors

Oksana Stalnov · Vitali Palei · Ilan Fono · Kelly Cohen · Avi Seifert

Received: 26 April 2006 / Revised: 5 January 2007 / Accepted: 5 January 2007 / Published online: 22 February 2007  
© Springer-Verlag 2007

**Abstract** The effectiveness of a small array of body-mounted sensors, for estimation and eventually feedback flow control of a D-shaped cylinder wake is investigated experimentally. The research is aimed at suppressing unsteady loads resulting from the von-Kármán vortex shedding in the wake of bluff-bodies at a Reynolds number range of 100–1,000. A low-dimensional proper orthogonal decomposition (POD) procedure was applied to the stream-wise and cross-stream velocities in the near wake flow field, with steady-state vortex shedding, obtained using particle image velocimetry (PIV). Data were collected in the unforced condition, which served as a baseline, as well as during influence of forcing within the “lock-in” region. The design of sensor number and placement was based on data from a laminar direct numerical simulation of the Navier-Stokes equations. A linear stochastic estimator (LSE) was employed to map the surface-mounted hot-film sensor signals to the temporal coefficients of the reduced order model of the wake flow field in order to provide accurate yet compact estimates of the low-dimensional states. For a three-

sensor configuration, results show that the estimation error of the first two cross-stream modes is within 20–40% of the PIV-generated POD time coefficients. Based on previous investigations, this level of error is acceptable for a moderately robust controller required for feedback flow control.

## 1 Introduction

An important area of active flow control (AFC) research involves the phenomenon of vortex shedding behind bluff bodies. These bodies typically serve some vital operational function, while aerodynamic efficiency is often sacrificed. Flow separates from large sections of the bluff body. In the case of a two-dimensional (2D) circular cylinder and above a critical Reynolds number ( $Re$ ) of about 47, a significant region of the near-wake is characterized by global flow instability (Gillies 1998). This instability results in asymmetrical vortex shedding, known as the von-Kármán (1954) vortex street, leading to increased drag, elevated noise levels, and flow-induced vibrations. The wake features are not highly sensitive to the details of the bluff-body geometry generating it (Roshko 1954). Developing an ability to control the wake of a bluff-body could reduce drag and unsteady-loads; increase mixing and heat transfer, and enhance combustion (Roussopoulos and Monkewitz 1996). The focus of the present research is on reducing the wake unsteadiness.

The Reynolds number regime currently studied corresponds to low Reynolds number, laminar and nominally two-dimensional wake. Beyond this range,

---

O. Stalnov · V. Palei · I. Fono · K. Cohen · A. Seifert  
Department of Fluid Mechanics and Heat Transfer,  
Faculty of Engineering, Tel-Aviv University,  
Tel Aviv 69978, Israel

K. Cohen  
KAYOS Enterprise Inc.,  
Colorado Springs, CO, USA

A. Seifert (✉)  
Meadow Aerodynamics Laboratory,  
Faculty of Engineering, Tel-Aviv University,  
Tel Aviv, Israel  
e-mail: seifert@eng.tau.ac.il

the nature of the vortex shedding transitions to several three-dimensional (3D) states as the Reynolds number increases (Williamson 1996). The critical  $Re$  for the onset of 2D vortex shedding of the present configuration was not determined; however, 2D vortex shedding was the dominant flow regime in all the data to be presented (e.g., Fig. 1). When active, open-loop, forcing of the wake is employed within the “lock-in” region (Blevins 1990), the wake vortices can be “locked” to the forcing frequency. Two-dimensional excitation within the “lock-in” regime increases the span-wise coherence and might strengthen the magnitude of the vortices, shorten the vortices’ formation length and consequently increase drag.

He et al. (2000) applied open-loop forcing to a cylinder boundary layer by rotation and demonstrated up to 60% drag reduction for Reynolds numbers of 200–1,000. Naim et al. (2006) investigated the flow around a circular cylinder at Reynolds numbers ranging from 40,000 to 280,000. A dominant vortex shedding frequency (VSF hereafter), was identified over the entire  $Re$  range. Using a single excitation slot that was moved around the circumference of the cylinder, effective open-loop AFC was performed. The flow “locked-in” to the excitation, using very low excitation amplitude in pulsed modulated mode and at frequencies of the same order as that of the natural VSF, even at  $Re = 100,000$ . In the “lock-in” regime, significant lift and drag increases were measured when the magnitude of the vortices in the near-wake was increased. On the other hand, the Drag was reduced at higher excitation frequencies, but this occurred when the boundary layer separation off the cylinder surface was delayed (also in He et al. 2000) and most probably not due to direct wake stabilization.

As opposed to other applications (e.g., boundary layer control with fixed separation region) where



**Fig. 1** A smoke flow visualization image showing baseline (unforced) vortex shedding off the D-shaped cylinder at  $Re = 150$

open-loop AFC approaches might be useful, unsteady wakes may effectively be controlled only using a feedback control system, as demonstrated for suppression of self-excited flow oscillations without geometry modification (Gillies 1998). Before proceeding into the details of modeling and control, it is imperative to appreciate the reasons as to why closed-loop control is of consequence and the main advantages associated with its implementation in flow control problems.

Closed-loop flow control is advantageous for the following reasons:

- Enables addressing problems that have not been solved using passive or open-loop active techniques (e.g., flow induced vibrations, boundary layer noise, turbulent drag reduction).
- Provides performance augmentation over an open-loop AFC system due to the sensing capability, especially at off-design conditions.
- Lowers the energy required to manipulate the flow and induce the desired behavior. This aspect affects actuation requirement and may be a deciding factor in marginal control authority cases (e.g., in a separation control experiment when the separation region is moving and multiple actuators could be used to optimally place the excitation at the mean separation location).
- Enables adaptability and robustness over a wider operating envelope, thereby enabling improved performance at multiple working points.

A comprehensive review of classical and modern feedback-flow-control approached is beyond the scope of this paper. The reader is referred to Collis et al. (2004) for this purpose. In this effort, the approach selected (on the route) to feedback flow control is based on the development of a low-dimensional model. Bluff-body wake flows, governed by the Navier-Stokes equations (NSE), are dominated by the dynamics of a relatively small number of characteristic large-scale spatial coherent structures, as observed experimentally in natural and periodically excited vortex sheets (Roussopoulos and Monkewitz 1996). A “full-state” model constructed for control purpose based on the NSE is not feasible for real-time estimation and control due to its high order. A desirable control system will, on the one hand, only measure a small number of surface-body sensors, estimate and control a small number of stationary large-scale spatial structures (“modes”) with time dependent mode amplitudes. On the other hand, it will keep the dimension of the wake flow low by not exciting it into a higher dimensional state, causing higher order modes to introduce instabilities, a phenomena referred to as spillover. In cases

where the complex spatio-temporal information could be characterized by a relatively small number of modes, (as in the 2D bluff-body wake prior to the bifurcation to 3D flow), model based feedback AFC can become computationally feasible. Therefore, to obtain a controller that can be implemented, a reduced-order model (ROM) is currently sought to represent the salient features of the flow field. The desired controller should provide effective feedback based upon information provided by a relatively small set of sensors. For low-dimensional control schemes to be implemented, a real-time estimation of the modes present in the wake is necessary since it is not possible to measure them directly, especially in real-time.

A common method used to reduce the model order is proper orthogonal decomposition (POD, Holmes et al. 1996). The POD method may be used to identify the characteristic features, or modes, of a bluff body wake as demonstrated by Gillies (1998) for the circular cylinder at  $Re \approx 100$ . This method is an optimal approach in that it will capture a larger amount of the flow energy in fewer modes than any other known decomposition of the flow (He et al. 2000). Low order modeling (LOM), based on POD techniques, is a vital building block in realizing a structured model-based closed-loop strategy for flow control.

Currently, PIV acquired velocity field data was fed into the POD procedure, to obtain the spatial modes, using the snapshots method (Sirovich 1987). The time histories of the temporal coefficients of the POD model are determined by applying the least-squares technique to the spatial eigenfunctions of the wake flow. Then, the estimation of the low-dimensional states (or mode amplitudes) is provided using linear stochastic estimation (LSE). This process leads to the state and measurement equations, required for design of the control system. Real-time estimation of the mode amplitudes will be provided for feedback control using the three surface-mounted sensors' information. For practical applications it is desirable to reduce the information required for estimation to the minimum. The requirement for the estimation scheme then is to behave as a modal filter that "combs out" the higher modes. The main aim of this approach is to thereby circumvent the destabilizing effects of observation "spillover" as described by Balas (1978). Spillover has been the cause for instability in the control of flexible structures and modal filtering was found to be an effective remedy (Meirovitch 1990).

The intention of the current strategy is that the signals, provided by a certain configuration of surface-mounted sensors placed on the upper surface of the D-shaped cylinder, are processed by the estimator to

provide the estimates of the first two, most energetic, periodic POD mode amplitudes. The estimation scheme, based on the LSE procedure introduced by Adrian (1977), predicts the temporal amplitudes of the first two POD modes from a small set of measurements obtained currently from experimental data. Surface-mounted sensors are always more practical to implement than wake or velocity field data. The LSE of POD modes was successfully applied by Cohen et al. (2005) for control of the Ginzburg-Landau wake model. Since the main aim of the current research was to experimentally validate a method successfully tested on numerical data (Cohen et al. 2006), LSE was used. However, future research will include dynamic estimators (Holmes 1996; Tadmor and Noack 2004) compared to the LSE approach. A major challenge lies in finding an appropriate number of sensors and determining locations that best enable the desired modal filtering. The need for modal filtering and the search for suitable sensor configuration is a problem common to the control of flexible structures, where a considerable research has been done (Baruh and Choe 1990; Lim 1997) and can be leveraged. Meirovitch (1990) provides a survey of several effective strategies.

Recent research on closed-loop control of the von-Kármán wake instabilities have addressed the issue of sensor number and placement based on non-intrusive sensors in the wake (Cohen et al. 2004). This approach may not always be implemented; therefore it is important to develop an effective method for body-mounted sensor number and placement. These sensors may measure surface pressures or (un-calibrated) time resolved skin friction, as is currently done. The advantages of surface-mounted sensors are:

- Simple, relatively inexpensive and reliable.
- Essential for real-life, closed-loop AFC applications where the direct measurement of the wake flow field is cumbersome (if not impossible).
- Enable "nearly collocated" sensors and actuators, which eliminate substantial phase changes (affects controller design).

In a recent study, Cohen et al. (2004) developed a sensor placement scheme based on the intensity of the spatial eigenfunctions obtained by applying the POD technique to 286 surface pressures for a D-shaped cylinder. The numerically generated data comprised 100 snapshots taken from the flow regime that corresponds to steady-state vortex shedding. A linear stochastic estimator (LSE) was employed to map the surface pressure signals to the mode amplitudes of the reduced order model of the wake flow field in order to provide accurate, yet compact estimates of the

low-dimensional states. For a four-sensor configuration, results show that the estimation errors of the first two modes are within 3–8% of the wake generated POD time coefficients. This error was further reduced to 1–3% using a six-sensor configuration. The main objective of the current research is to experimentally validate the sensor placement approach developed by Cohen et al. (2004) using surface-mounted hot-films placed on the upper surface of a D-shaped cylinder in a wind tunnel.

The remainder of the paper is structured as follows: the experimental setup is described in Sect. 2. This is followed, in Sect. 3, by a description of the low-dimensional POD model based on the PIV generated wake data. Then, in Sect. 4, based on the POD model, a surface-mounted sensor configuration is used to estimate the first two, periodic, cross-stream velocity mode amplitudes. The uncertainties associated with real-life sensor signals for estimation are discussed. Finally, Sect. 5 provides conclusions of the current research and some recommendations for future work.

## 2 Experimental set up and $St-Re$ correlation

The experiments were performed at the 2 ft by 3 ft low-speed, low-turbulence, closed-circuit wind tunnel at the Meadow Aerodynamics Laboratory at Tel-Aviv University. This tunnel is especially suitable to perform very low speed experiments. The flow uniformity and stability is maintained at speeds as low as 0.1 m/s. The motor RPM was monitored and found to vary less than 5% at speeds below 1 m/s. The free-stream velocity was measured by recording the VSF of a 4 mm diameter circular cylinder located at the upper part of the test section entrance, upstream of the model. Using the well known Strouhal–Reynolds correlation (Williamson 1996) over the  $Re$  range for which the correlation was constructed, it is possible to extract the free-stream velocity from the shedding frequency only, using an iterative process. This method is also in a very good agreement with the free-stream velocity determined from the PIV measurements. A Pitot tube is connected to an extremely sensitive pressure transducer that is capable of measuring velocities above 1 m/s. Very good agreement was found between the three methods in the overlap region.

The test section is instrumented with a traversing system, capable of positioning two hot-wires in the boundary layers and wake of the D-shaped cylinder. The four walls of the test section are made from optical quality glass for flow visualization and PIV. A commercial 3D PIV system is currently used in 2D mode to acquire the stream-wise wake velocity field. The system

includes a double-pulsed Nd-Yag laser at a maximum output of 200 mJ per pulse and a repetition rate up to 15 Hz. Seeding particles were provided by a theatrical fog generator located downstream of the test section and upstream of the fan. An articulated arm with a set of mirrors and a light sheet forming optics mounted at the exit routed the laser pulses to above the test section and generated a thin (about 2 mm wide) light sheet in the near wake of the D-shaped cylinder. A double exposure CCD camera with a resolution of 1 k by 1 k pixels captured the image pairs required for the PIV analysis. Natural vortex shedding was measured in a phase-locked manner. The trigger signal in the baseline flow was provided by a hot-wire measuring the vortex shedding velocity signal about 10 mm to the side of the laser light sheet in the near wake. When the flow was forced, the low frequency amplitude modulation (AM) excitation TTL signal was used as a phase reference. “Lock-in” was assured by monitoring an identical frequency and constant phase lag between the excitation and the wake hot-wire signals.

Figure 1 shows the von-Kármán vortex street in the wake of an unforced D-shaped cylinder at  $Re \approx 150$  (based on its thickness). For the current study, a D-shaped cylinder was selected so that the separation points will be fixed, and to assure study of direct wake control, with fixed width, rather than mixed separation and wake control. An inherent benefit of an elongated D-shaped cylinder is the suitability to implant internal Piezo fluidic actuators and keep the dominant dimension (i.e., body thickness) very small such that low  $Re$  number experiments could be performed in air, while always injecting the excitation at the fixed separation points.

The D-shaped cylinder, shown in Fig. 2a–d, is a semi-ellipse 46.2 mm long and 6.5 mm thick. A closed-loop flow control system is comprised also of an actuation system that introduces perturbations into the flow, to obtain a desired state alternation. The approach of the current research is to rely on internal cavity based fluidic actuators similar to those used by Yehoshua and Seifert (2006), due to applicability considerations.

In the 6.5 mm thickness of the D-shape, two layers of 15 Piezo-electric fluidic actuators were placed. Each actuator spans 30 mm (with 0.5 mm spacing between each actuator pair) and is separately addressable. The fluidic output from nominally 0.5 mm wide, 45° directed excitation is controllable in the range of 0 to about 5 m/s at the actuator’s resonance frequency of  $1.2 \pm 0.1$  kHz. Low frequency excitation, corresponding to the natural VSF, is generated by amplitude modulating (AM) the actuators’ resonance frequency. Currently, sensor measurements were provided by

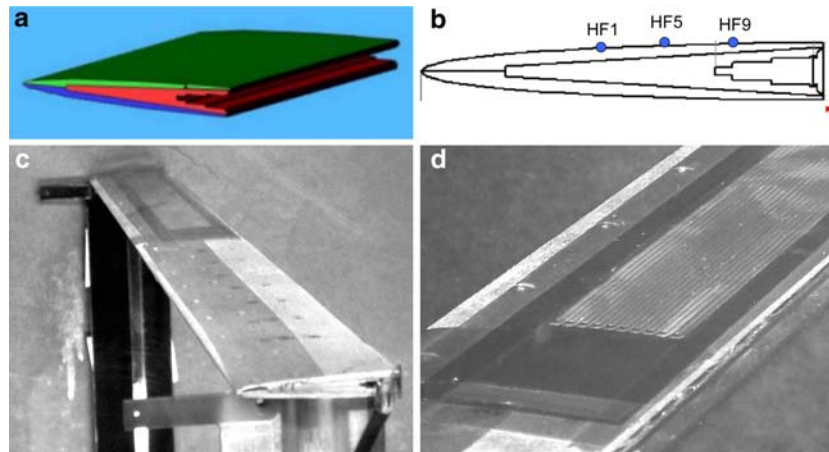


**Fig. 2** **a** Solid model of D-shaped cylinder showing its three main components. The core (red) is made of stainless steel and houses two rows of 15 Piezo fluidic actuators each, two aluminum made skins are bolted to the core and form the external semi-elliptic shape and the actuator slots at the trailing edges. The slots are segmented, allowing individual operation of each actuator. Thickness is 6.5 mm at the trailing edge, length is 46.2 mm and span is 580 mm. **b** A cross section of the D-shaped cylinder model. Thickness is 6.5 mm at the trailing edge, length is 46.2 mm. Fifteen actuator slots are located on each corner of the upper and lower surface trailing edge. Nominal slot width is

0.5 mm and it is oriented at about 45° away from the surface, facing downstream. Hot-films marked by HF9, 5 and 1 above are located 11, 19 and 27 mm from the trailing edge, respectively. **c** The D-shape is installed in the 2 by 3 ft low speed tunnel at Tel-Aviv University. The flow is from left. The array of 10 hot-films is seen on the upper surface with its leads routed to the far side. **d** A close rear view of the hot-films array. Sensor spacing is 2 mm. The actuator slots can be seen on the trailing edge upper side junction. Sensing was applied only on the upper surface while actuation was operated only from the lower surface actuator slots

three body-mounted hot-films. Surface pressures could also, in principle, be used for sensing but for the current study they lack sensitivity and require complex installation as compared to hot-films. An array of 10 hot-films (HF), mounted on the upper side of the model were placed close to the tunnel center-plane and were spaced 2 mm apart in their stream-wise location. The hot-films were operated in constant-temperature mode (over-heat ratio of 1.2) and sampled at high frequency (1.35 kHz) by a computerized data acquisition system. Typical data acquisition sequence contained all hot-films, hot-wires, tunnel conditions (velocity, fan rpm and temperature) sampled for at least 20 seconds. Phase-locked data were acquired for the hot-films, PIV and excitation signal, when the actuators operated in open-loop inside the “lock-in” region. “Lock-in” is determined by the inspection of the stationary relative phase between the excitation signal and all relevant sensor signals and by a clear dominant peak of the excitation frequency in all measured sensors. Currently, only three of the hot-films were used for this study, as illustrated in Fig. 2b–d. Due to the low hot-film signal-to-noise ratio (SNR, –12.5 dB for HF 9) during the main part of the study, resulting from the very low speed and instrumentation noise, ensemble-averaging technique was used to improve the SNR. The number of realizations that were averaged and its effect on the quality of the estimation

process is studied and discussed. Subsequently the hot-films SNR was significantly improved, for future real-time feedback AFC experiments.

A typical feature of vortex shedding at low  $Re$  is manifested in the  $St$ - $Re$  correlation. Vortex shedding frequencies were measured in the near-wake of the D-shape while velocities were measured by using the circular cylinder  $St$ - $Re$  correlation from Williamson (1996). Figure 3 shows the  $St$ - $Re$  relationship for the

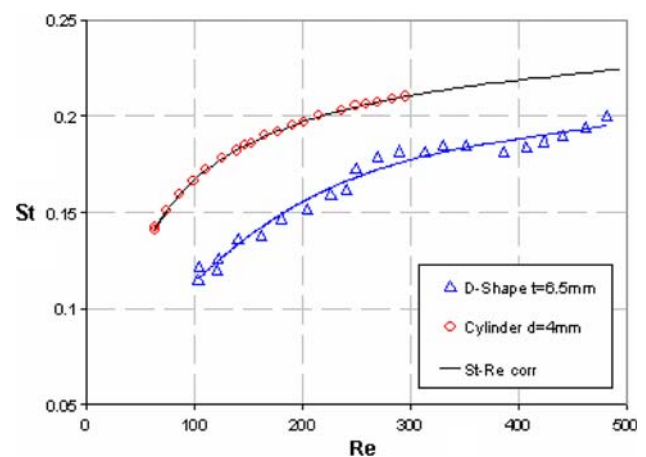


**Fig. 3** Strouhal–Reynolds numbers correlation for the 4 mm circular cylinder (used to measure the free-stream velocity) and for the 6.5 mm thick D-shaped cylinder. The black line is a correlation from Williamson (1996)

current D-shaped cylinder wake, compared to the correlation of a circular cylinder. It can be noted that the  $St$  for the D-shape lies below the universal correlation. This is due to the presence of thick boundary layers on the D-shaped cylinder as compared to their thinner counterparts on a circular cylinder. Increasing the length scale used to calculate both  $St$  and  $Re$  for the D-shape collapses the current data to the universal correlation. The discontinuities in the D-shape  $St$ - $Re$  relationship for  $Re > 250$  are probably related to 3D bifurcation which were not studied yet in detail and were avoided by limiting the  $Re$  range in the current study to remain below 250.

### 3 POD modeling of excited flow

Feasible real-time estimation and control of a bluff body wake may be effectively realized by reducing the complexity of the wake flow field by using the POD techniques. This model reduction approach is referred to in the literature as the Karhunen-Loeve expansion (Holmes et al. 1996). The ideal POD model will contain an adequate number of modes to enable modeling of the temporal and spatial characteristics of the large-scale coherent structures inherent in the flow, but no more modes than absolutely necessary. The MATLAB based POD and LSE algorithms used in this effort are based on those developed for previous work done at the USAF Academy (Cohen et al. 2005).

Figure 4 shows the dominant VSF measured in the near wake of the D-shape at  $Re = 152$  using a hot-wire, while the hot-wire was traversed in the vertical ( $z$ )

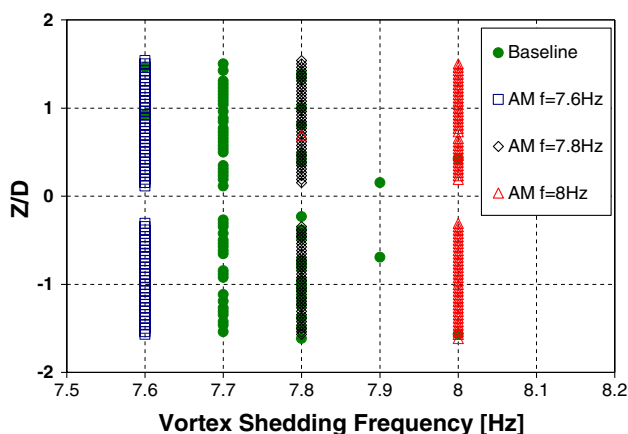


**Fig. 4** Vortex shedding frequency for the D-shape at  $Re = 152$  versus the vertical position in the wake,  $x/D = 7$  from the trailing edge. Note that the excitation was introduced only from the lower surface actuators. Duration of such measurement is about 30 min. Low frequency is generated by amplitude modulation (AM) of the 1.26 kHz actuators resonance frequency by low frequency that is close to the natural VSF

direction to cross the entire wake. For the baseline case there is a scatter of about  $\pm 0.1$  Hz in the VSF, outside the frequency-doubling region in the  $0.25 < z/D < 0.25$  range. When AM-forcing was applied from the lower actuator slot, with uniform phase across the span, at frequencies that are  $\pm 0.2$  Hz away from the natural VSF, perfect “lock-in” was obtained, as can be seen from the shift of the dominant frequency. For all of those cases the relative phase between the excitation and the wake-edge hot-wire was stationary. Currently, the wake flow field, represented by the cross-stream velocity component was obtained from wind tunnel PIV data of the D-shaped cylinder wake at  $Re = 225$ . Sixteen datasets, consisting of 20 image pairs each, were acquired at equal phase increments along the excitation cycle. Each data set (for a given phase) was then ensemble-averaged, generating one representative “snapshot” of the excited flow. The minimum number of snapshots was determined by acquiring 40 image pairs in a certain phase, calculating the norm of the  $V$ -velocity in each snapshot and calculating the averaged norm of increasing number of snapshots. It was found that the averaged norm of 20 snapshots changed in less than 1% (of the averaged norm) when additional snapshots were averaged. Figure 5a presents a typical snapshot resulting from the above procedure. These 16 snapshots were then used for the POD analysis. The data were acquired after ensuring that the cylinder wake (frequency, amplitude and phase of the vortex shedding with respect to the excitation signal) reached steady state, by observing and recording hot-wires and hot-film signals along with the excitation signal. For control design purposes, the POD method enables the flow, depicted in this study by the cross-stream velocity, to be modeled as a set of ordinary differential equations (ODE) as detailed by Holmes et al. (1996). First, the flow field data is loaded and arranged from the PIV data of the D-shaped cylinder wake, in accordance with their relative phase with respect to the excitation signal. The decomposition of this component of the velocity field is as follows:

$$\tilde{v}(x, y, t) = V(x, y) + v(x, y, t) \quad (1)$$

where  $V$  denotes the mean flow and  $v$  is the fluctuating component that may be expanded as:

$$v(x, y, t) = \sum_{k=1}^n a_k(t) \phi_i^{(k)}(x, y) \quad (2)$$

where  $a_k(t)$  denotes the time-dependent coefficients (TC) and  $\phi_i(x, y)$  represents the non-dimensional

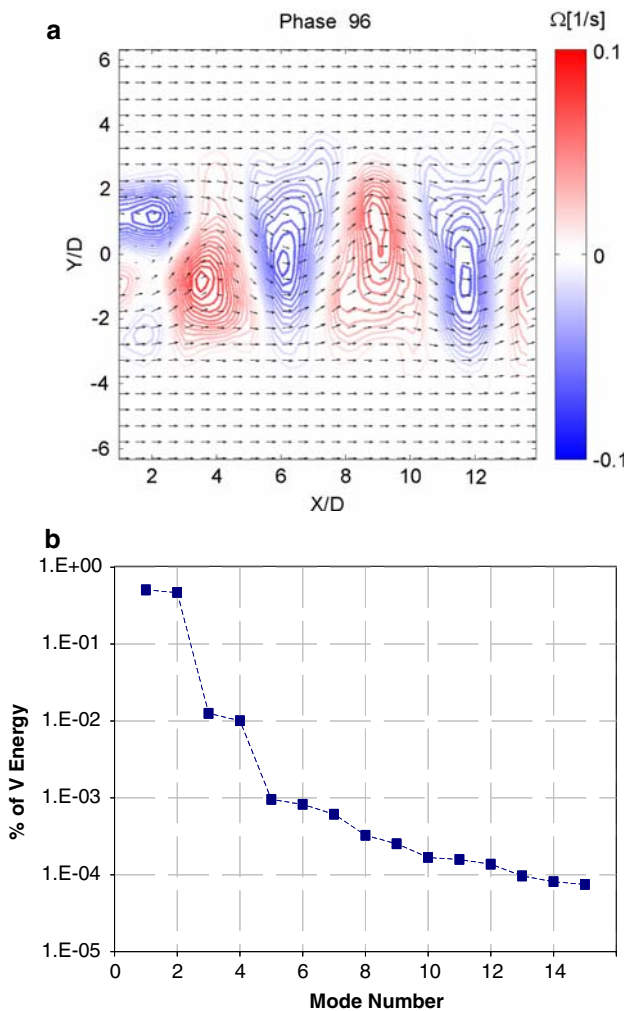


**Fig. 5** **a** Phase-locked “snapshot” showing velocity vectors and vorticity contours (every 2nd vector is shown, the difference between contours levels is 0.005 1/s). Flow excitation with AM signal ( $F_m = 13.65$  Hz and  $F_c = 1,200$  Hz), natural VSF = 13.5 Hz,  $Re = 225$ . **b** The decay rate of the PIV generated V-velocity Eigenvalues

spatial eigenfunctions of the velocity determined from the POD procedure. From an ensemble of snapshots, the “mean snapshot” is computed and then this mean is subtracted from each member of the ensemble. This is done primarily for scaling reasons; i.e., the deviations from the mean contain information of interest but may be small compared with the total signal.

Figure 5a shows one ensemble-averaged snapshot, PIV measured velocity vectors and vorticity contours at a given phase along the excitation cycle, at  $Re = 225$ . The excitation Strouhal number ( $St$ ) is 0.16 (based on the excitation frequency of 13.65 Hz, free-stream velocity of 0.54 m/s and the actual D-shape model thickness). This length scale is used, disregarding the effective wider near-wake (with which the VSF scales)

due to the boundary layer thickness. The PIV velocity uncertainty for this data set is  $\pm 3\%$  of the free-stream velocity. Sixteen such equally spaced phases were acquired for one excitation cycle.

Next, the empirical correlation matrix was computed, using the inner product, defined as  $(u, v) \equiv \int dx u(x) \cdot v(x)$ , where both  $u$  and  $v$  refer to the cross flow velocity component. Solving the eigenvalue problem, the eigenvalues and the orthogonal spatial eigenfunctions,  $\phi_i(x, y)$ , were obtained. Since the eigenvalues measure the relative energy of the system dynamics contained in each mode, they may be normalized to correspond to a percentage of the system energy. For the current working point ( $Re \approx 225$ ), the eigenvalues for the V-velocity are presented in Table 1. Note that the overwhelming portion of the energy associated with the POD modes, after the mean has been removed, is contained in the first two modes (97.2%).

Finally, the time histories of the temporal coefficients (TC’s) of the PIV generated POD model,  $a_k(t)$ , were determined using the extracted spatial modes and the phase-locked (to the excitation signal) snapshots of the flow. However, it is not possible to obtain a direct real-time measurement of  $a_k$ , which is why it needs to be estimated from direct measurements such as body-mounted sensors. An important aspect of reduced order modeling for feedback AFC applications concerns truncation. How many modes are important and what are the criteria for effective truncation? The answers to the above questions have been addressed by Cohen et al. (2003). That numerical study demonstrated that control of the POD model of the von-Kármán vortex street in the wake of a circular cylinder at low Reynolds numbers ( $Re \approx 100$ ) was viable using just the first mode. Furthermore, feedback based on the first mode alone significantly attenuated all the other modes in the four-mode POD model.

In view of the above result, currently, truncation of the POD model can take place after the first two modes, which contain over 97% of the V-velocity energy containing fraction, as seen in Table 1. Figures 6 and 7 illustrate the eigenfunctions of the first four modes for both  $u$  and  $v$ , respectively. At this point, it is

**Table 1** Eigenvalues of wake V velocity from PIV data and POD analysis,  $Re = 225$ , using 16 ensemble averaged snapshots

Mode	Velocity (V) POD eigenvalues
1	0.504
2	0.468
3	0.012
4	0.010

**Fig. 6** PIV-measured U-velocity PIV-POD modes, D-shape,  $Re = 225$ ,  $St = 0.16$  (13.65 Hz), *broken line indicates negative values*

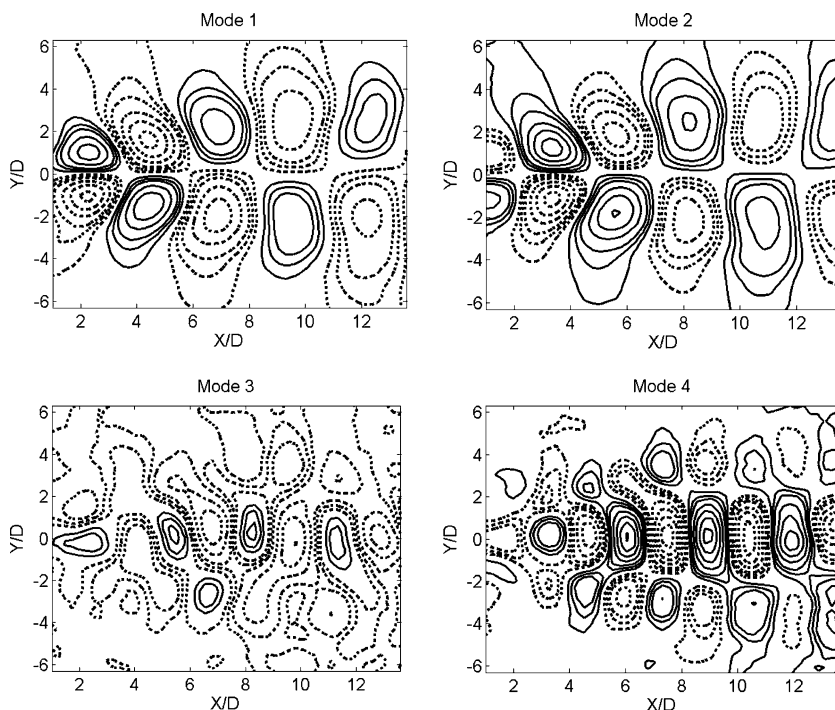
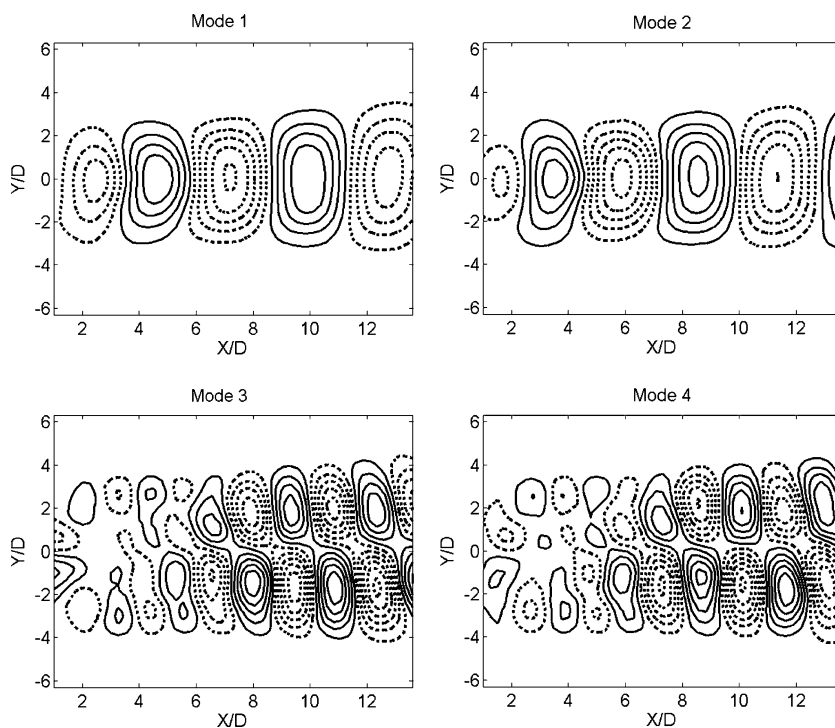


**Fig. 7** PIV measured V velocity PIV-POD modes, D-shape,  $Re = 225$ ,  $St = 0.16$  (13.65 Hz), *broken line indicates negative values*



imperative to note the difference between the number of modes required to reconstruct the flow and the number of modes required for effective low-dimensional modeling for control design purpose. In this study, we were interested in estimating only those modes required for closed-loop flow control. On the

other hand, a more accurate reconstruction of the velocity (and pressure) field, based on a low-dimensional model, may be obtained using between four to fifteen modes. The number of required modes may also change with the flow feature to be modeled and controlled, especially in 3D cases.



The quintessential question is whether an effective estimate of the states, of the two mode low-dimensional model coefficients,  $a_k$ , can be estimated based on a small number of surface-mounted sensors. The answer is affirmative and the details that provide the estimate of the first two modes,  $a_1 - a_2$ , are presented in the next section. The first four PIV-POD time coefficients (TC) for the V-velocity are shown in Fig. 8a. Note the relative magnitudes, as indicated also in Table 1, and the different frequency of TC 3–4 compared to TC 1–2. Even though the 3rd and 4th TC are at twice the fundamental VSF, linear stochastic estimation (LSE) will be able to predict TC 3–4, with sufficient number of sensors and superior SNR. However, it might not be needed if the energy is concentrated in modes 1–2, as currently is the case, even when the control loop will be closed.

On the other hand, a POD model is, strictly speaking, only valid for the flow situation from which it was derived. Deane et al. (1991) looked at Reynolds number effects on the POD modes of the wake of a

circular cylinder at  $Re = 100-200$ . They present direct evidence that the cylinder modes, unlike those of a pressure driven cavity flow, change significantly with Reynolds number, and that modes developed at one  $Re$  are not useful at off-reference  $Re$  for the cylinder. Therefore, it is expected that any modification of the flow field by means of feedback AFC may bring about a reduction and in some cases absolute nullification of the validity of the model. In order to address this problem, modified POD models have been proposed by Noack et al. (2003), Tadmor et al. (2004a, b) and Siegel et al. (2003), while experimental validation was not performed yet.

#### 4 Estimation, sensor configuration and results

The time histories of the temporal coefficients of the flow field V-velocity in the current study were determined by introducing the POD spatial eigenfunctions into the flow field data using the least-squares technique. The intent of the applied strategy is that the measurements provided by the body-mounted hot-film sensors are processed by the estimator to provide the estimates of the first two temporal modes of the wake flow field cross-stream velocity. The estimation scheme, based on the LSE procedure introduced by Adrian (1977), estimates the temporal amplitudes of the first  $n$  (currently  $n = 2$ ) POD modes from a finite set of hot-film measurements obtained from the experiment of the controlled open-loop forced D-shaped cylinder wake. All the measurements were acquired only after ensuring that the cylinder wake flow regime converged to steady state vortex shedding inside the “lock-in” regime. The mode amplitudes,  $a_1 - a_2$ , were mapped onto the extracted sensor signals from the body-mounted sensors,  $u_s$ , as follows:

$$a_n(t) = \sum_{s=1}^{m=3} C_s^n u_s(t) \quad (3)$$

where  $m$  is the number of sensors and  $C_s^n$  represents the coefficients of the linear mapping. The effectiveness of a linear mapping between wake velocity measurements and POD states has been experimentally validated by Cohen et al. (2004). The coefficients  $C_s^n$  ( $n = 1, 2; s = 1, 2, 3$ ) in Eq. (3) are obtained via the LSE method from the set of discrete sensor signals and temporal, PIV generated POD time mode coefficients,  $a_1 - a_2$ .

The issue of sensor placement and number has been dealt with in an ad-hoc manner in published studies concerning closed-loop flow control (Cohen et al.

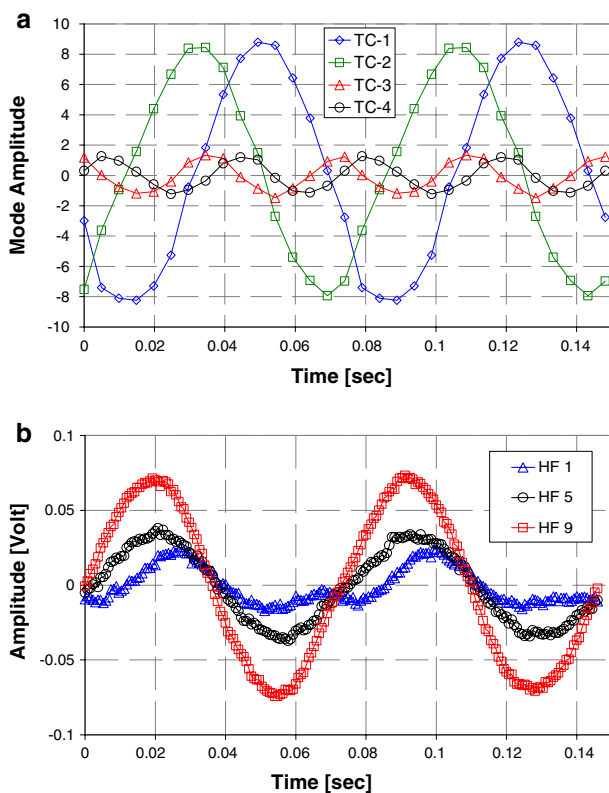


**Fig. 8** **a** POD modes' time coefficients (TC) generated from PIV-measured vertical velocity component (V). The first two modes are at the same frequency as the modulating frequency of the input signal to the Piezo fluidic actuators. Excited flow,  $Re = 225$ . The total time of the data presented is equal to two cycles of the fundamental excitation frequency. **b** Ensemble averaged (90 cycles) hot film signals. Conditions as those of Figs. 5, 6, 7. HF locations shown in Fig. 2b

2006). For effective closed-loop control system, the following questions need to be answered:

- How many sensors are required?
- Where should the sensors be located?
- What are the criteria for judging an effective sensor configuration, and
- Is the configuration robust?

Note that we seek to arrive at an “effective sensor configuration” as it is based on validated heuristics as opposed to “optimal sensor configuration” that results from a mathematically optimal pattern search for a sensor configuration. So, what needs to be done to determine an effective sensor configuration is to find the areas of energetic modal activity.

The selection of the sensor configuration in this paper is based on the findings of an earlier effort by Cohen et al. (2006), as cited above. The knowledge concerning the spatial eigenfunctions obtained from the POD procedure provides insight into where the modal activity is high. It was found that the most effective locations for surface-mounted sensors for estimation of modes 1 and 2 were around the trailing edge of the D-shaped cylinder. This is where the surface-mounted hot-film sensors are placed in the current effort (see Fig. 2b).

Three hot-film sensors were placed at the upper surface of the cylinder near the trailing edge. These sensors target modes 1 and 2 of the wake V-velocity component. The time histories of the three hot film sensors are presented in Fig. 8b. These signals are ensemble averaged, containing about 90 vortex-shedding cycles, in order to improve the SNR. Ensemble averaging was needed since the signal to noise ratio of the preliminary raw HF data acquired for this effort was very low (Fig. 11). After ensemble averaging, it is evident that the VSF dominates the spectrum of the HF sensors. Also there is a decay of the signal as one propagates from the trailing edge towards the leading edge and a phase shift develops. These are encouraging findings in the prospects that the signals are well correlated to the TC and on the other hand, not too similar to each other.

Subsequently, the LSE procedure was applied to obtain the transformation matrix  $C_s^n$  and to obtain the estimates of the V-velocity/surface-mounted hot-film signals POD mode coefficients. The estimated versus actual mode amplitude plot, for the current three-sensor configuration are presented in Fig. 9. The similarity between the original and estimated signals is evident and very encouraging. However quantification is needed and this was performed by considering the normalized difference, as detailed below.

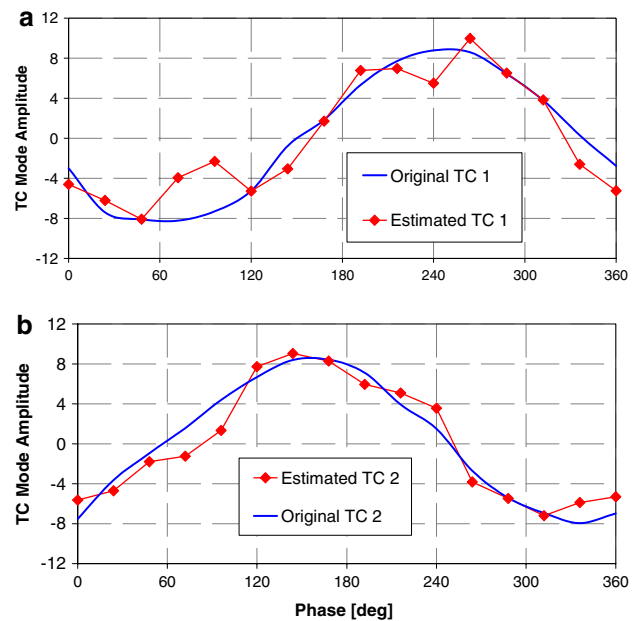


**Fig. 9** Time coefficients (TC) mode amplitudes resulting from POD analysis of the PIV-measured V-velocity, modes 1 and 2 shown (termed “Original”) compared with their estimation from the 3 surface-mounted hot-films (termed “estimated”)

The normalized difference was calculated between the actual wake mode amplitude, extracted from the PIV data by the POD procedure and the estimates obtained from the LSE procedure. For convenience, the absolute difference is normalized by the actual PIV extracted mode amplitudes of the “trainer” data and presented as a percentage in Fig. 10. The comparison

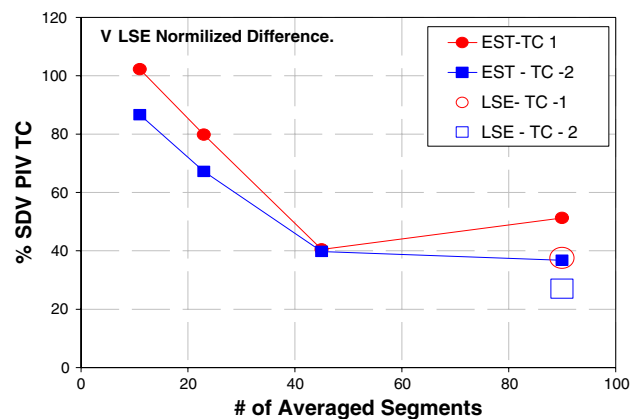


**Fig. 10** The normalized difference between the “original” (according to the caption of Fig. 9) V-velocity POD time coefficients of modes 1 and 2 and their estimation from 3 surface-mounted hot-films, using the “trainer” data (empty symbols) and a different set of hot-film data (“estimator”, marked “EST” in the above legend) versus the number of data segments (each corresponding to one VSF cycle) taken into the ensemble averaging process

between the original PIV-POD TC 1 and TC 2 and the “training” data estimation also suffers from the low SNR, and the resulting differences are 37 and 27%, for modes 1 and 2, respectively, using 90 vortex shedding cycles for the estimator data. When using a different data set from the hot-film sensors for estimation, and lowering the number of ensemble averaged cycles as well, the estimator error increases to about 50 and 40% for TC 1 and TC 2, respectively. While a reduction to 20 ensemble averaged cycles, roughly doubles the error, which is expected due to the  $1/\sqrt{n}$  ( $n$  is the number of cycles averaged) converging ratio. Although the RMS error may appear to be high, the frequency content and the phase obtained using the LSE procedure appears to be very good. The resulting error and the number of sensors may be integrated together into a cost function. The purpose of the design process would then be to select the configuration that minimizes this cost function. Considering the fact that the LSE is providing V-velocity estimates of the wake flow field, the RMS values appear to be adequate and can be used for closed-loop flow control using a moderately robust controller (Fig. 11).

Considering the fact that the entire database used for the current wake modes estimation is for forced data, one should consider the probability that the observability of the baseline POD modes would be lower. Therefore, the baseline hot-film sensor and wake hot-wire readings were recorded and processed as well. It was found that it did not significantly differ from the signals currently used for the estimation of the excited flow. The magnitudes were slightly higher in the excitation flow, as expected.

To overcome the low-SNR found during the preliminary stages of this study, a significant effort was invested in eliminating the noise sources from contaminating the HF signals. A result of the HF9 signal after significant hardware modifications is presented in Fig. 12. This signal represents a 26 dB improvement of

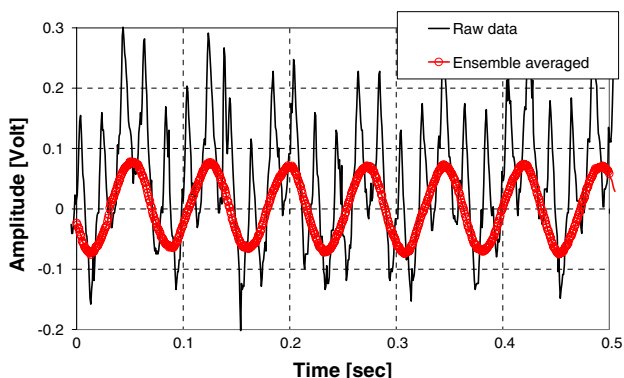


**Fig. 11** Raw “Locked data” of hot-film 9 before ensemble averaging and after 90 segments ensemble averaged processing

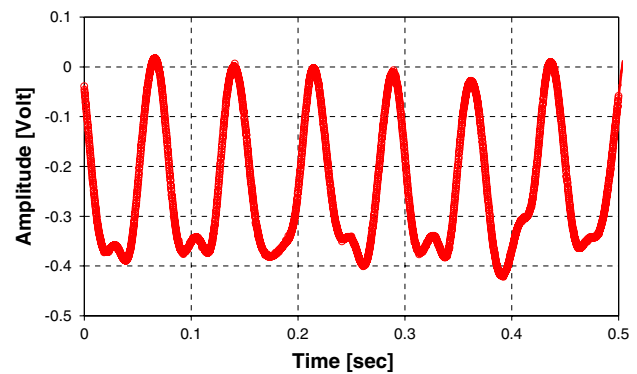


**Fig. 12** Improved SNR HF-9 showing raw data.  $Re = 225$ .  $St = 0.16$  ( $Fl = 13.5$  Hz)

the SNR as compared to the raw HF data acquired prior to the modification (e.g., from  $-12.5$  to  $+13.4$  dB). Such a signal quality could be used for real-time estimation of the most energetic POD wake modes from a small-set of three hot-film sensors.

The current use of LSE is a possible shortcoming of the method. Non-linear methods such as dynamic estimators (Gerhard et al. 2003; Rowley and Juttijudata 2005; Luchtenburg et al. 2006) could be used and compared with the results of LSE.

## 5 Conclusions and recommendations

This paper provides a first experimental validation of a heuristic procedure for the placement and number of body-mounted sensors for feedback flow control of a D-shaped cylinder wake, based on proper orthogonal decomposition modeling. The design used surface readings obtained from hot film sensors to estimate POD mode time coefficients of the wake flow field (cross-stream velocity) at a  $Re = 225$ . The results show that the estimates of the first two modes of the wake flow field are accurate to within 35% RMS error, with respect to the measured POD time coefficients RMS. This level of error is acceptable for a moderately robust closed-loop flow controller.

Further research will aim at examining sensitivity of the developed heuristic procedure for sensor number and placement, to noise and to variations in Reynolds number. Furthermore, the effectiveness of the sensor configuration will be examined for variable open-loop steady-state and transient forcing conditions. Also, dynamic estimators could be used instead of linear stochastic estimators used in conjunction with band pass filters rather than ensemble averaging. Finally, it is required to examine the performance of the current closed-loop flow control strategy at increased Reynolds

numbers, beyond the bifurcation to 3D vortex shedding pattern.

**Acknowledgments** The authors would like to acknowledge the support and assistance provided by TAU technical staff, Tomer Bachar, Shlomo Paster, Shlomo Moshel, Shlomo Blivis, Eli Kronish, Avram Blas, Eli Nevo, Mark Vasserman and TAU Meadow Aerolab students and staff.

## References

- Adrian RJ (1977) On the role of conditional averages in turbulence theory. In: *Turbulence in liquids*, Proceedings of the fourth biennial symposium, Rolla, Mo., September 22–24, 1975. (A77-40426 18-34) Princeton, NJ, Science Press, pp 323–332
- Balas MJ (1978) Active control of flexible systems. *J Optim Theory Appl* 25(3):217–236
- Baruh H, Choe K (1990) Sensor placement in structural control. *J Guid Control* 13(3):524–533
- Blevins RD (1990) *Flow induced vibration*, 2nd edn. Van Nostrand reinhold, New York, pp 451
- Cohen K, Siegel S, McLaughlin T, Gillies E (2003) Feedback control of a cylinder wake low-dimensional model. *AIAA J* 41(8):000–1452
- Cohen K, Siegel S, Luchtenburg M, and McLaughlin T, Seifert A (2004) Sensor placement for closed-loop flow control of a ‘D’ shaped cylinder wake. 2nd AIAA flow control conference, 28 June to 1 July 2004, Portland, Oregon, AIAA-2004-2523
- Cohen K, Siegel S, Wetlesen D, Cameron J, Sick A (2004) Effective sensor placements for the estimation of proper orthogonal decomposition mode coefficients in von-Kármán vortex street. *J Vib Control* 10(12):1857–1880
- Cohen K, Siegel S, McLaughlin T, Gillies E, Myatt J (2005) Closed-loop approaches to control of a wake flow modeled by the Ginzburg-Landau equation. *Comput Fluids* 34(8):927–949
- Cohen K, Siegel S, McLaughlin T (2006) A heuristic approach to effective sensor placement for modeling of a cylinder wake. *Comput Fluids* 35(1):103–120
- Collis S, Joslin RD, Seifert A, Theofilis V (2004) Issues in active flow control: theory, simulation and experiment. *Prog Aero Sci* V40:237–289 (previously AIAA paper 2002–3277)
- Deane AE, Kevrekidis IJ, Karniadakis GE, Orsag SA (1991) Low dimensional models for complex geometry flow: application to grooved channels and circular cylinder. *Phys Fluids A* 3:2337–2354
- Gillies EA (1998) Low-dimensional control of the circular cylinder wake. *J Fluid Mech* 371:157–178
- He JW, Glowinski R, Metcalfe R, Nordlander A, Periaux J (2000) Active control and drag optimization for flow past a circular cylinder. *J Comput Phys* 163:83–117
- Holmes P, Lumley JL, Berkooz G (1996) *Turbulence, coherent structures, dynamical systems and symmetry*. Cambridge University Press, Cambridge
- Lim KB (1997) A disturbance rejection approach to actuator and sensor placement. NASA CR-201623, January–February
- Meirovitch L (1990) *Dynamics and control of structures*. Wiley, New York, pp 313–351
- Naim A, Greenblatt D, Seifert A, Wagnanski I (2006) Active control of cylinder flow with and without a splitter plate using piezoelectric actuators. *AIAA Paper* 2002–3070, June 2002. (Submitted to flow, turbulence and combustion, 2006)
- Noack BR, Afanasiev K, Morzynski M, Tadmor G, Thiele F (2003) A hierarchy of low-dimensional models for the transient and post-transient cylinder wake. *J Fluid Mech* 497:335–363
- Roshko A (1954) On the drag and shedding frequency of two-dimensional bluff bodies. *NACA TM* 3169
- Rowley CW, Juttijudata V (2005) Model-based control and estimation of cavity flow oscillations. *IEEE conference on decision and control*
- Gerhard J, Pastoor M, King R, Noack BR, Dillmann A, Morzynski M, Tadmor G, (2003) Model-based control of vortex shedding using low-dimensional Galerkin models. *AIAA paper* 2003–4262
- Luchtenburg M, Tadmor G, Lehmann O, Noack BR, King R, Morzynski M (2006) Tuned POD galerkin models for transient feedback regulation of cylinder wake. *AIAA paper* 2006–1407
- Roussopoulos K, Monkewitz, PA (1996) Nonlinear modeling of vortex shedding control in cylinder wakes. *Physica D* (97):264–273
- Siegel S, Cohen K, McLaughlin T (2003) Feedback control of a circular cylinder wake in experiment and simulation. 33rd AIAA fluid dynamics conference, Orlando, AIAA 2003–3569
- Sirovich L (1987) Turbulence and the dynamics of coherent structures. *Quart Appl Math* XLV:561–571
- Tadmor G, Noack BR, Morzynski M (2004a) Low-dimensional models for feedback flow control. Part I: empirical Galerkin models. 2nd AIAA flow control conference, 28 June–1 July 2004, Portland, Oregon, AIAA-2004–2408
- Tadmor G, Noack BR, Morzynski M, Siegel S (2004b) Low-dimensional models for feedback flow control. Part II: Observer and controller design. 2nd AIAA flow control conference, 28 June to 1 July 2004, Portland, Oregon, AIAA Paper 2004–2409
- Tadmor G, Noack BR (2004) Dynamic estimation for reduced Galerkin models of fluid flows. Paper WeM18.1, Proceedings of the 2004 American control conference, Boston, USA, June 30 to July 2, 2004
- von-Kármán T (1954) *Aerodynamics: selected topics in light of their historic development*. Cornell University Press, New York
- Williamson CHK (1996) Vortex dynamics in the cylinder wake. *Annu Rev Fluid Mech* 8:477–539
- Yehoshua T, Seifert A (2006) Boundary condition effects on the evolution of a train of vortex pairs in still air. *Aeronaut J* 110(1109):397–417